Journal of GeoEngineering, Vol. 11, No. 1, pp. 13-25, April 2016
http://dx.doi.org/10.6310/jog.2016.11(1).2

AN APPROACH TO ESTIMATE REQUIRED GEOSYNTHETICS STRENGTH IN REINFORCED SLOPES WITH INCLINED BACKSLOPE FOR STATIC AND SEISMIC LOADING

Castorina Silva Vieira[1]

ABSTRACT

An approach to estimate the required strength of geosynthetics in reinforced earth structures with inclined backslope under static and seismic loading conditions is presented in this paper. The results were achieved with a developed algorithm, based on pseudo-static limit equilibrium analyses, that assumes a two-part wedge failure mechanism. Design charts to obtain equivalent earth pressure coefficients and potential failure surfaces are presented. Given the slope angle, the backslope angle, the design value of the soil friction angle, the height of the slope, the unit weight of the soil and the seismic coefficients, one can determine the required strength of geosynthetics for structure equilibrium. This paper intends to broaden the available design charts for geosynthetic reinforced earth structures with non-horizontal backslopes under static and seismic loading, as well as, to provide a helpful tool to design preventive measures for unstable slopes. These charts are also particularly useful for those cases in which the classical earth pressure theories underestimate the required force for slope equilibrium.

Key words: Reinforced steep slopes, geosynthetics, pseudo-static analyses, earth pressure coefficients, seismic loading, inclined backslope.

1. INTRODUCTION

The construction of an embankment with slopes steeper than the naturally stable angle requires additional stabilising forces. These forces can the provided by horizontal reinforcements layers placed inside the embankment (geosynthetics) or by a heavy facing system (such as gabions or large rocks). The results herein presented can be applied to the internal design of geosynthetic reinforced steep slopes, as well as, to the design of a stable facing system under static and seismic loading conditions.

In the last decades some methods have been proposed for the internal design of geosynthetic stabilised structures. These methods can be grouped into three different approaches. The first approach, usually limited to reinforced soil slopes, is an extension of the classical limit equilibrium slope stability methods (methods of slices) with the inclusion of the reinforcement forces (Wright and Duncan 1991; FHWA 2010; Ghanbari and Ahmadabadi 2010; Yang *et al*. 2011, 2013). The second approach is based on considerations of limit equilibrium, such as two-part wedge or logarithmic spiral analyses (Schmertmann *et al*. 1987; Jewell 1989; Ling *et al*. 1997; Ling and Leshchinsky 1998; Vieira *et al*. 2011; Basha and Basudhar 2010). The third is a kinematic approach of limit analysis and can be performed considering a continuum medium, through the soil and reinforcement homogenization, or two separated structural components—soil and reinforcement components (Michalowski 1998; Ausilio *et al*. 2000). This paper follows the second approach.

The horizontal resultant force due to lateral earth pressures that should be supported by the reinforcement layers or by the facing system to ensure the structure equilibrium is usually determined by limit equilibrium analyses. The failure surface associated with the maximum value of this horizontal force defines the critical surface.

The effect of the seismic loading on the required force for slope equilibrium could be based on pseudo-static analyses. These analyses are, frequently, considered as conservative since transitory earthquake acceleration is assumed to act permanently on the structure. A proper selection of the seismic coefficients used in the pseudo-static analyses shall compensate for the conservatism of these methods. On the other hand, this conservatism may counterbalance the acceleration amplification when not implicitly considered in the design.

This paper presents updated results from a developed computer program, based on limit equilibrium analysis, able to estimate the required strength for slope equilibrium under static and seismic loading conditions (Vieira *et al*. 2011; Vieira *et al*. 2013; Vieira 2014).

Simplified equations to estimate earth pressure coefficients for static and seismic design of geosynthetic reinforced structures were previously proposed by Vieira *et al*. (2011) but these equations, as the majority of the published results, are limited to horizontal backslopes. In this paper the effect of the inclined backslope is introduced.

The design of geosynthetic reinforced steep slopes is often based on design charts, such those proposed by Schmertmann *et al*. (1987) and Jewell (1989) for static conditions or those proposed by Michalowski (1998) and Vieira *et al*. (2011) for seismic loading conditions. However, these design charts are limited to horizontal backslopes. The main purpose of this paper is to broaden the available design charts to determine the required strength for the equilibrium of slopes with non-horizontal backslopes. These charts are a really helpful tool particularly for those cases in which Coulomb's earth pressure theory (Coulomb 1776)

Manuscript received October 13, 2015; revised January 25, 2016; accepted March 9, 2016.

[1] Professor (corresponding author), University of Porto-Faculty of Engineering, Department of Civil Engineering, Rua Dr. Roberto Frias, 4200-465 Porto, Portugal (e-mail: cvieira@fe.up.pt).

and Mononobe-Okabe theory (Okabe 1924; Mononobe and Matsuo 1929) could underestimate earth pressure coefficients.

2. LIMIT EQUILIBRIUM APPROACH

The two-part wedge failure mechanism is, as mentioned before, one of the limit equilibrium approaches suitable for the evaluation of the required force for equilibrium of unstable slopes. With regard to geosynthetic reinforced structures, this failure mechanism does not consider explicitly the interaction between the soil and the geosynthetics. However, numerical simulations carried out by Vieira *et al*. (2013) have shown that required geosynthetic strength evaluated by limit equilibrium methods provides a good estimate for the minimum required strength for slope stability. These simulations have also shown that, at failure of the reinforced steep slope, the maximum shear strains in the backfill occur very close to the potential failure surface estimated by the two-part wedge failure mechanism.

In view of the inclusion of seismic loading effects, the failure mechanism will be introduced as pseudo-static limit equilibrium approach. The horizontal and vertical seismic inertial forces, acting at the centre of gravity of the potential failure soil mass, are considered through the horizontal and vertical seismic coefficients, k_h and k_v, expressed as fractions of the gravitational constant, g. The convention adopted in this paper is that a positive horizontal seismic coefficient, $+k_h$, corresponds to a seismic inertial force acting outward and a vertical seismic coefficient, $+k_v$, corresponds to a seismic inertial force acting downward.

In the two-part wedge mechanism, the potential sliding soil mass is divided in two blocks (Fig. 1). In this paper a vertical inter-wedge potential failure surface was assumed. Although some authors (Jewell 1989) have considered that a vertical and smooth (no vertical shear force between the two wedges) inter-wedge boundary lead to conservative results, Vieira *et al*. (2013) have shown that a two-part wedge failure mechanism with a vertical inter-wedge boundary is not a factor of conservatism. The conservatism of the results comes from the assumption of a smooth inter-wedge surface.

The force P_{ae}, schematized in Fig. 1 at the face of the structure, represents the minimum value of the required force, which should be supported by the reinforcement layers, to ensure structure equilibrium (*i.e.,* to ensure a stabilizing force equal to the horizontal component of the unstable force).

Usually, the horizontal component of the earth pressure coefficient is the parameter used in the analysis of facing stability or reactive force in reinforcements, hence the required force for equilibrium, P_{ae}, was considered horizontal. The inter-wedge force was considered by its horizontal and vertical components, H_1 and V_1, related by the following equation:

$$V_1 = \lambda H_1 \tan\phi \tag{1}$$

where λ is the inter-wedge mobilized shear stress ratio (a user defined variable) and ϕ is the soil internal friction angle. The effect of the direction of the inter-wedge force, expressed by λ, on the equivalent earth pressure coefficient, K_{req}, was analysed by Vieira *et al*. (2013). These authors found that a horizontal inter-wedge force ($\lambda = 0$) is very conservative, moreover, since it is assumed the full mobilization of the soil shear strength along the failure surfaces OA and AB (Fig. 1), to be consistent, the present study considers $\lambda = 1$ (soil shear strength fully mobilized in the inter-wedge vertical surface).

Obviously, the geometry of the blocks that leads to the maximum value of the required force for equilibrium, *i.e.*, the geometry shown in Fig. 1, is not known. Thus a computer code was developed to find the most critical failure surface, that is to say the one that leads to the maximum horizontal force required for slope equilibrium, P_{ae}.

To find the critical failure surface the software creates a square mesh of points, with lateral side equal to the height of the structure and spacing between points equal to 1% of the mesh side. For each of these points (represented by point A in Fig. 1), several potential failure surfaces are analyzed, ranging the angle θ_1 (see Fig. 1) from θ_2 to 90° with increments of 0.1°.

The two-part wedge failure mechanism degenerates to a single wedge with a plane failure surface when this mechanism is more adverse (for instance when the slope face is near vertical).

The equilibrium equation, on horizontal direction, of the forces acting on wedge 1 (Fig. 1), taking into consideration the relation between the horizontal and vertical components of the inter-wedge force stated by Eq. (1), provides the horizontal component of the inter-wedge force, H_1:

$$H_1 = \frac{(1 \pm k_v) + k_h \cdot \dfrac{\tan\phi \sin\theta_1 + \cos\theta_1}{\sin\theta_1 - \tan\phi \cos\theta_1}}{\lambda \tan\theta_1 + \dfrac{\tan\phi \sin\theta_1 + \cos\theta_1}{\sin\theta_1 - \tan\phi \cos\theta_1}} \cdot W_1 \tag{2}$$

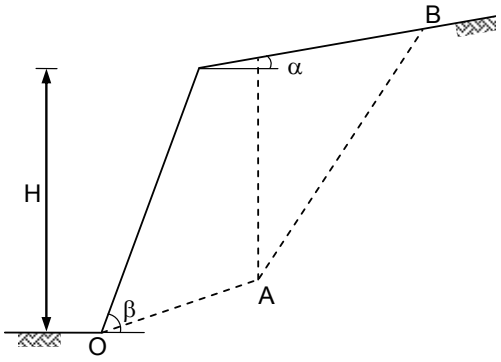

(a) Geometric characteristics of the slope

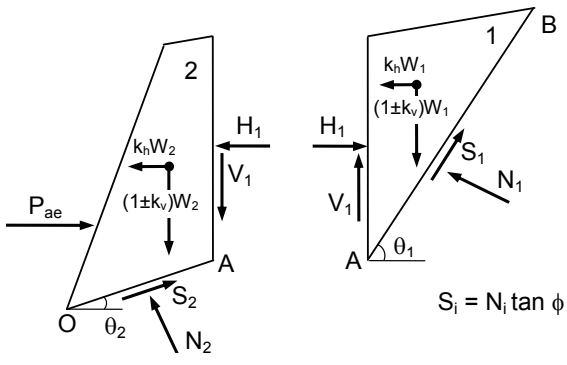

(b) Two-part wedge failure mechanism

Fig. 1 Potential failure surface

Known the horizontal component of the inter-wedge force, H_1, the required force for equilibrium, P_{ae}, for each potential failure surface, can be calculated by the equilibrium, on horizontal direction, of the forces acting on wedge 2, with the equation:

$$P_{ae} = H_1 + k_h W_2 - \frac{\tan\phi\cos\theta_2 - \sin\theta_2}{\tan\phi\sin\theta_2 + \cos\theta_2}\cdot\left[(1 \pm k_v)W_2 + V_1\right] \quad (3)$$

The bilinear failure surface, to which corresponds the maximum value of P_{ae} is considered the critical failure surface.

For static conditions, the need of reinforcement or the need of the facing system to reach the slope equilibrium is usually represented by an earth pressure distribution. By the similarity between critical potential failure surfaces, Terzaghi (1943) demonstrated that the earth pressure distribution at the back of a wall increases, like a hydrostatic pressure, in simple proportion to depth.

Most design suggestions available for geosynthetic stabilised slopes under seismic conditions (Ausilio *et al*. 2000; Nouri *et al*. 2008; Vieira *et al*. 2011) assume the linear (increasing with depth) distribution of reinforcement force. Furthermore, numerical analyses carried out by Bathurst and Hatami (1998) and Vieira *et al*. (2006) showed that for walls with a sliding base, dynamic loads increase in a generally linear fashion with depth bellow the crest of the wall. Therefore, assuming that the earth pressures increase linearly with depth, the required force for slope equilibrium, P_{ae}, could be expressed by:

$$P_{ae} = \frac{1}{2} K_{req}\gamma H^2 \quad (4)$$

where K_{req} is an equivalent earth pressure coefficient, γ is the soil unit weight and H is the slope height. The results will be expressed, in sequence, by the equivalent earth pressure coefficient. This earth pressure coefficient, K_{req}, can be used to determine the required tensile strength of the reinforcement layers.

For a given vertical spacing between reinforcement layers, S_v , a reinforcement with a proper allowable strength should be selected, to provide at each depth an available stress greater than the required stress for equilibrium (evaluated with K_{req}). This means that the available stress (provided by the reinforcements) must equal or exceed the required stress at every depth, or in terms of forces:

$$T_d \geq K_{req}\gamma z S_v \quad (5)$$

where T_d represents the design value of the reinforcement strength per unit width and z the depth of the reinforcement layer.

Note that when vertical seismic acceleration is considered, the equivalent earth pressure coefficient, K_{req}, is not equal to the Mononobe-Okabe earth pressure coefficient (Okabe 1924; Mononobe and Matsuo 1929), K_{ae}, even for a structure with vertical face. For the particular case of structures with vertical face, the critical failure surface degenerates to a single wedge surface, coincident with the one assumed by the Mononobe-Okabe approach, but the equivalent earth pressure coefficient, K_{req}, is equal to:

$$K_{req} = (1 \pm k_v)K_{ae} \quad (6)$$

where k_v represents the vertical seismic coefficient.

3. RESULTS AND DISCUSSION

3.1 General Aspects

The results presented in this paper regards purely frictional materials, with internal friction angle in the range of 20° ~ 45°, slope angles between 40° and 90°, backslope angles in the range 0° ~ 18.4°, zero pore water pressure (r_u = 0) and a competent foundation.

The effect of the seismic loading on the required force for slope equilibrium was based on a pseudo-static analysis. In the parametric analysis, the horizontal seismic coefficient was considered in the range 0 ~ 0.30. The vertical seismic loading was considered through a vertical seismic coefficient, k_v, defined as a function of the horizontal seismic coefficient, k_h. The ratio k_v / k_h has assumed values of +1.0, +0.5, −0.5 and −1.0. When the vertical inertial forces act downwards, k_v is considered a positive value.

3.2 Results for Static Loading

The effect of the backslope angle on the equivalent earth pressure coefficient, K_{req}, as a function of the slope angle, β, considering frictional materials with ϕ equal to 30º and 40º is illustrated in Fig. 2. The backslope angle was expressed in Fig. 2 by the ratio of the vertical to the horizontal distances (V : H).

The effect of the backslope angle on the required force for equilibrium seems to increase with slope angle, β. Assuming a friction angle, ϕ, equal to 30° (Fig. 2(a)) , the equivalent earth pressure coefficient, K_{req}, increased approximately 23% and 29% when the backslope ranges from horizontal to an angle of 18.4°, for β = 60° and β = 80°, respectively. These variations decreased to 11% and 18%, respectively, for a friction angle of 40° (Fig. 2(b)). Thus it can be concluded that the effect of the backslope on the required force for equilibrium decreases with the soil friction angle and is more significant for steeper slopes.

Figure 3 illustrates the effect of soil friction angle on critical failure surfaces for embankments with slope angles of 60° (Fig. 3(a)) or 80° (Fig. 3(b)) and a backslope angle of 11.3° (1V : 5H). As expected the volume of soil potentially in failure decreases with the soil friction angle. While the potential failure surfaces for β = 60° are bilinear (Fig. 3(a)), for the steeper slope the critical failure surfaces become planar (Fig. 3(b)) and coincident with those admitted in Coulomb's earth pressure theory (Coulomb 1776).

Figure 3(a) provides evidence that the Coulomb's earth pressure theory is not suitable to estimate the potential failure surface for an embankment with slope angle of 60°. The potential failure surface reached with the two-part wedge failure mechanism (T-W) (to which corresponds the maximum value of the horizontal force for slope equilibrium-critical failure surface) and the planar failure surface assumed in the Coulomb's earth pressure theory, for β = 60° and soil friction angle of 30° are illustrated in Fig. 4. The values of the equivalent earth pressure coefficient obtained by the developed code (Fig. 2(a)) and the value estimated by Coulomb's theory are also included in Fig. 4. Comparing these values it can be concluded that Coulomb's earth pressure theory underestimates around 14% the required force for slope equilibrium.

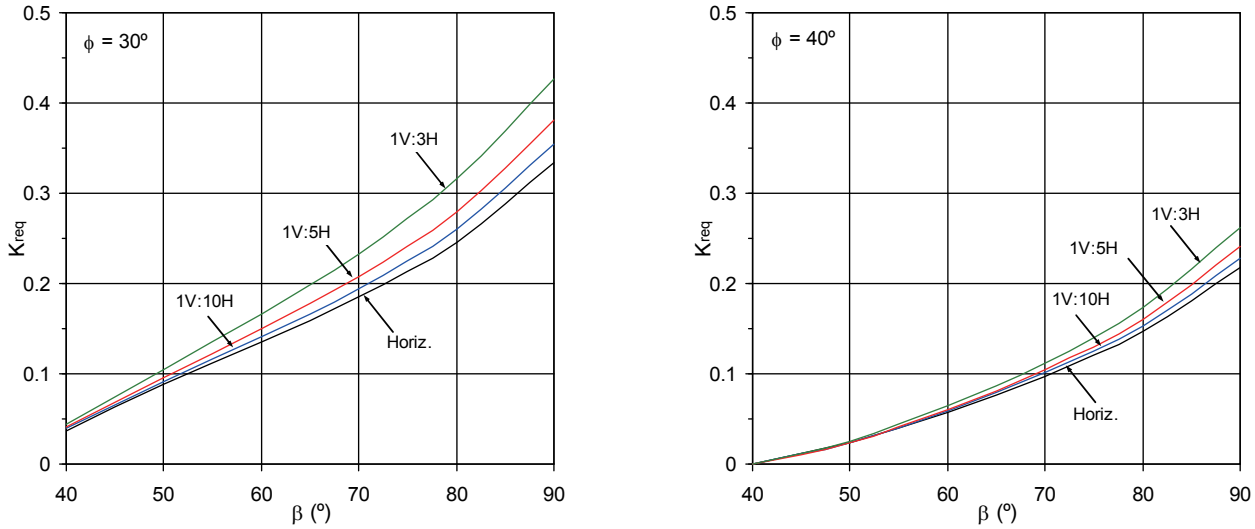

(a) Soil friction angle, ϕ = 30° (b) Soil friction angle, ϕ = 40°

Fig. 2 Effect of the backslope angle on the required force for equilibrium

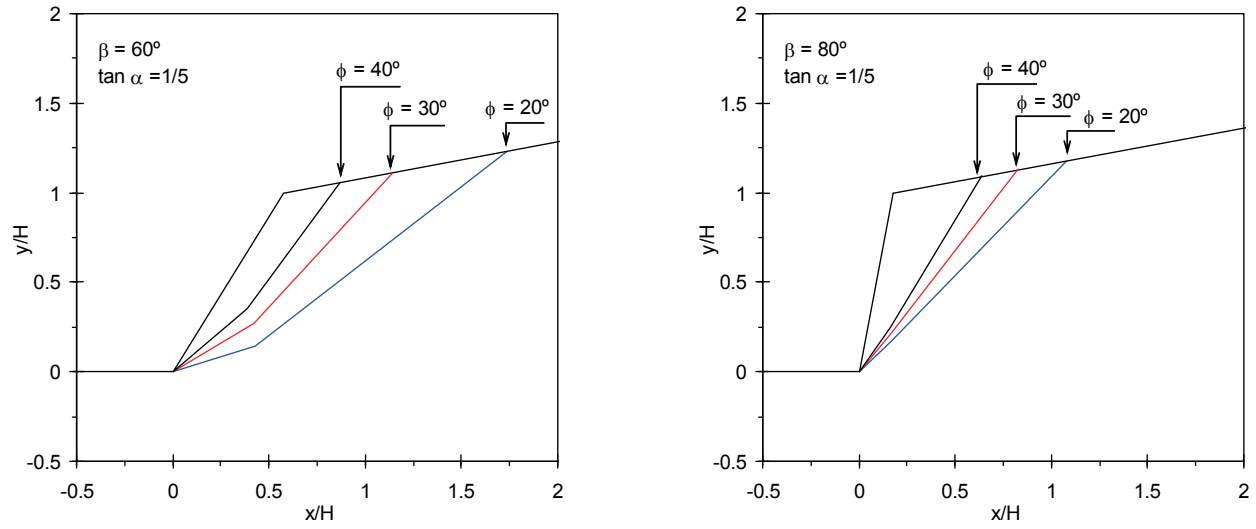

(a) Slope angle, β = 60° (b) Slope angle, β = 80°

Fig. 3 Effect of soil friction angle on critical failure surfaces for backslope angle, $\alpha = \tan^{-1}(1/5)$

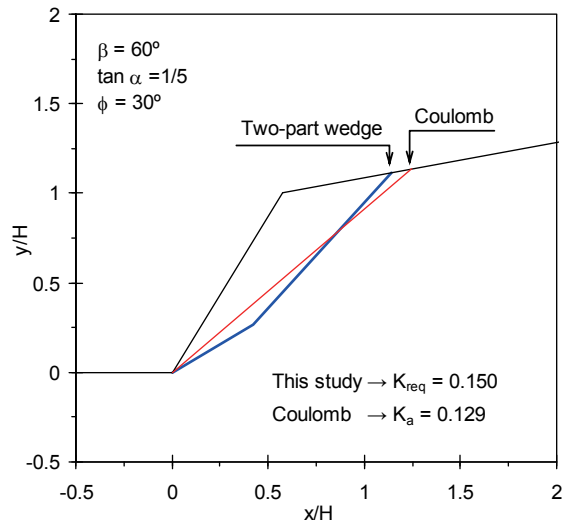

Fig. 4 Comparison of the critical failure surface achieved by the T-W mechanism with that admitted by Coulomb's theory, $\beta = 60°$; $\alpha = \tan^{-1}(1/5)$

When the slope angle, β, is not close to 90°, Coulomb's earth pressure theory should not be used to estimate the value of K_{req}, since it does not correspond to the maximum value of the horizontal force to reach the slope equilibrium. Based on this evidence, Vieira (2014) has proposed a simplified approach that provides an extension of the Coulomb earth pressure theory to the stability analyses of steep slopes. For static loading conditions, the equivalent earth pressure coefficient can be estimated by (Vieira 2014):

$$K_{req}^{aprox} = \left[\frac{\sin(\beta-\phi)}{\sin\beta\left(1+\sqrt{\frac{\sin(\phi-\alpha)\cos(\beta-\phi)}{\sin(\beta-\alpha)}}\right)} \right]^2 \times\left[1+\cos\beta\cos(\beta-\phi)\cos(\beta-\alpha)\right] \quad (7)$$

where β is the slope angle, α is the backslope angle and ϕ is the bakcfill internal friction angle.

3.3 Effect of Horizontal Seismic Loading

The effect of the horizontal seismic coefficient, k_h, on the equivalent earth pressure coefficient for structures with slope face inclined at 60° and 80° and backslope angle of 11.3° (1V : 5H) is represented in Fig. 5. As expected, the greater the horizontal seismic coefficient, the larger the horizontal force for slope equilibrium. Comparing the values of K_{req} for seismic loading with those obtained for static conditions (k_h = 0), the increase induced by the seismic action is higher for the flatter slope. For instance, assuming ϕ equal to 30°, the increment of K_{req} induced by a horizontal seismic loading with k_h = 0.3 is, approximately, 257% and 152% for β = 60° and β = 80°, respectively. However, it should be noted that these increases do not represent the real increments of the required force for slope equilibrium induced by the seismic action. The partial safety factors considered in the seismic design are usually lower than those used in static conditions.

Figure 6 illustrates the effect of the horizontal seismic coefficient, k_h, on critical failure surfaces for slopes with 60° (Fig. 6(a)) and 80° (Fig. 6(b)), backslope angle of 11.3° (1V : 5H) and soil friction angle equal to 30°. Not unexpectedly, the volume of soil potentially in failure increases with the horizontal seismic coefficient. Although, the rate of increase of soil volume is greater than that of the horizontal seismic coefficient, k_h.

The critical failure surfaces for the steeper slope illustrated in Fig. 6(b) are coincident to those estimated by the Mononobe-Okabe earth pressure theory. For the flatter slope (β = 60°), the potential failure surface is not linear and Mononobe-Okabe theory underestimates the unstable soil volume and consequently, the required force for slope equilibrium (Fig. 7).

Figures 8 to 11 summarize the required force for slope equilibrium (expressed by K_{req}) for horizontal seismic coefficient equal to 0 (static loading), 0.1, 0.2 and 0.3, assuming slope angles in the range 40° ~ 90° and backfill material with an internal friction angle between 20° and 45°. Figure 8 refers to structures with horizontal backslope and Figs. 9, 10 and 11 are referring to backslope angles of 5.7°, 11.3° and 18.4°, respectively.

3.4 Effect of Vertical Seismic Loading

In the particular case of the design of geosynthetic reinforced steep slopes, the effect of the vertical component of seismic action is not explicitly considered in the generality of the codes (AASHTO 2002; FHWA 2010; NCMA 1998; JRTRI 1999). For some of them, the consideration of a vertical seismic coefficient infers that the maximum values of the vertical and the horizontal components of the seismic action occur simultaneously. Some results are presented in this study to clarify the real effects of neglecting the vertical seismic action on the required force for slope equilibrium.

As mentioned in 3.1, the vertical seismic loading is considered through a vertical seismic coefficient, k_v, defined as a function of the horizontal seismic coefficient, k_h. For the ratio k_v / k_h, values of +1.0, +0.5, −0.5 and −1.0 were considered. The sign of k_v is positive when the corresponding vertical inertial forces act downwards.

Figure 12 shows the effect of k_v on the required force for slope equilibrium, expressed by the equivalent earth pressure coefficient, K_{req}, for slope angles, β, equal to 60° and 80°, horizontal backslope and an horizontal seismic coefficient, k_h equal to 0.2. For comparison purposes, it is also represented the equivalent earth pressure coefficient for static conditions ($k_h = k_v = 0$).

When vertical inertial forces act downwards ($k_v > 0$) the required force for slope equilibrium increases (comparatively to the force demanded when $k_v = 0$). The effect of k_v seems also to increase with the slope angle. For the steeper slope (Fig. 12(b)), the increase induced by k_v is almost independent of the backfill friction angle. For β = 60°, the effect of k_v seems to slightly decrease with ϕ.

The effect of k_v on the required force for slope equilibrium for non-horizontal backslope is illustrated in Fig. 13. Figure 13 refers to structures with slope angle, β, equal to 60° and 80°, backslope angle of 11.3° (1V : 5H) and an horizontal seismic coefficient, k_h equal to 0.2.

For the two slope angles under analysis (β = 60° and β = 80°), when soil friction angle is low (ϕ ≤ 25°) and the vertical inertial forces act upwards ($k_v < 0$), the required force for slope equilibrium exceeds the value for $k_v = 0$ (and also the value for $k_v > 0$). This trend is the opposite of the evidence illustrated in Fig. 12, for structures with horizontal backslope (greater required force for slope equilibrium when $k_v > 0$).

In order to explain this behaviour for soils with low shear strength, Fig. 14 illustrates the effect of the vertical seismic coefficient on the critical failure surface for a structure with slope angle equal to 60°, backslope angle of 11.3° (1V : 5H), k_h = 0.2 and considering the soil friction angle equal to 25° (Fig. 14(a)) or 30° (Fig. 14(b)). Regardless of soil friction angle, when the vertical inertial forces act upwards ($k_v < 0$), the volume of soil potentially in failure is larger than the corresponding soil failure volume for $k_v = 0$. The highest values of the required force for equilibrium when $k_v < 0$ and ϕ = 25° (Fig. 13(a)), comes from the large increase of the weight of the soil potentially in failure (Fig. 14(a)). Even with the weight reduction induced by the upwards vertical inertial force, the vertical force $(1 - k_v)W$ (see Fig. 1(b)) is larger than the weight of the soil potentially in failure when $k_v = 0$. Thus, the required force for slope equilibrium, P_{ae}, when $k_v < 0$ exceeds the value achieved for $k_v = 0$.

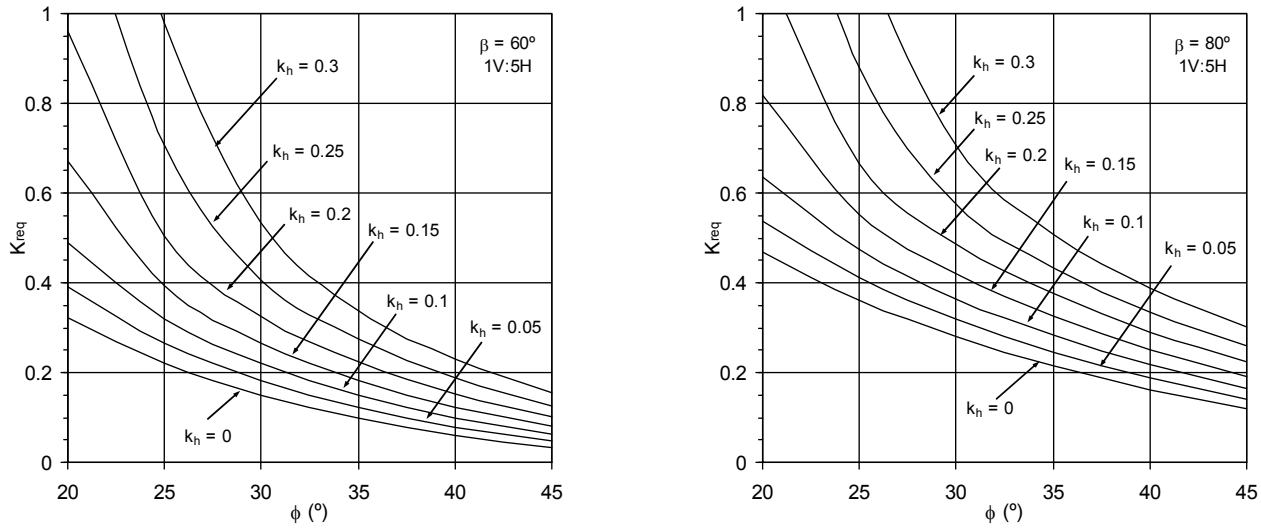

(a) β = 60°, α = $\tan^{-1}$(1/5) (b) β = 80°, α = $\tan^{-1}$(1/5)

Fig. 5 Effect of the horizontal seismic coefficient, k_h, on the earth pressure coefficient

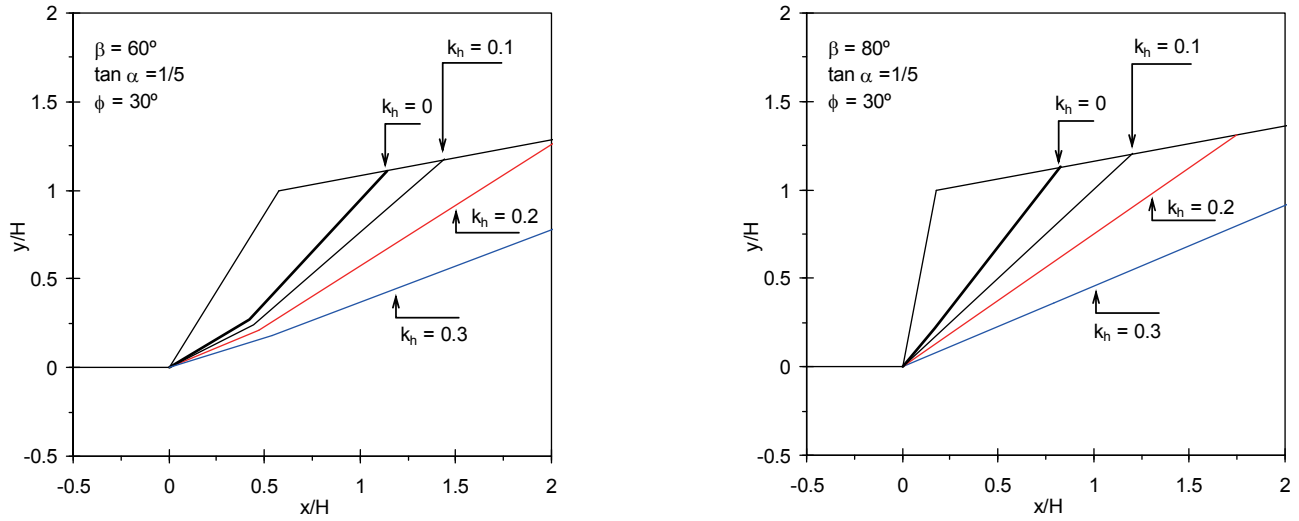

(a) Slope angle, β = 60° (b) Slope angle, β = 80°

Fig. 6 Effect of the horizontal seismic coefficient, k_h, on critical failure surfaces for backslope angle, α = $\tan^{-1}$ (1/5) and ϕ = 30°

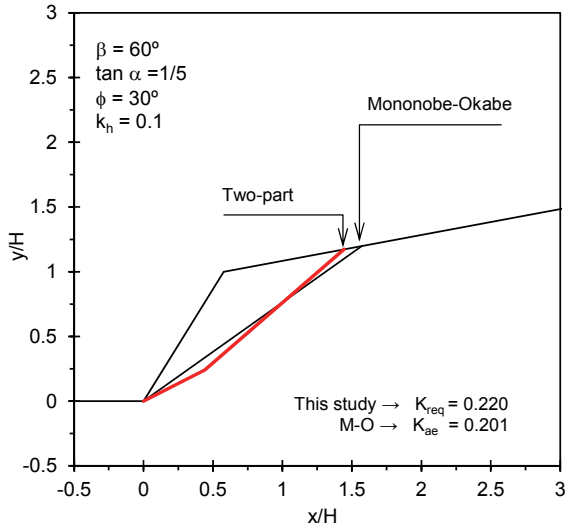

Fig. 7 Comparison of the critical failure surface achieved with the developed code with the Mononobe-Okabe failure surface, β = 60°; α = $\tan^{-1}$ (1/5)

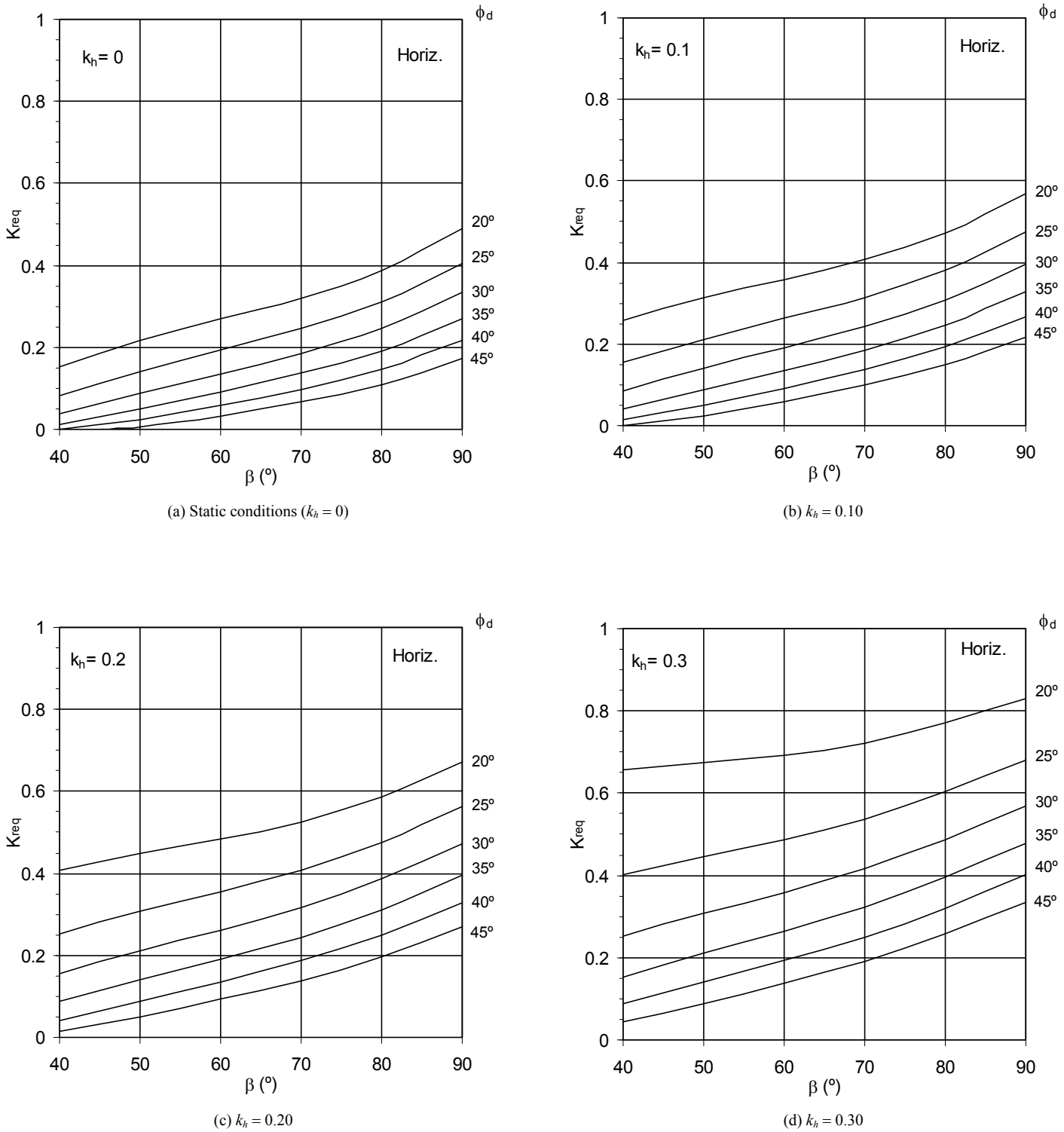

(a) Static conditions ($k_h = 0$)

(b) $k_h = 0.10$

(c) $k_h = 0.20$

(d) $k_h = 0.30$

Fig. 8 Design charts for slopes with horizontal backslope

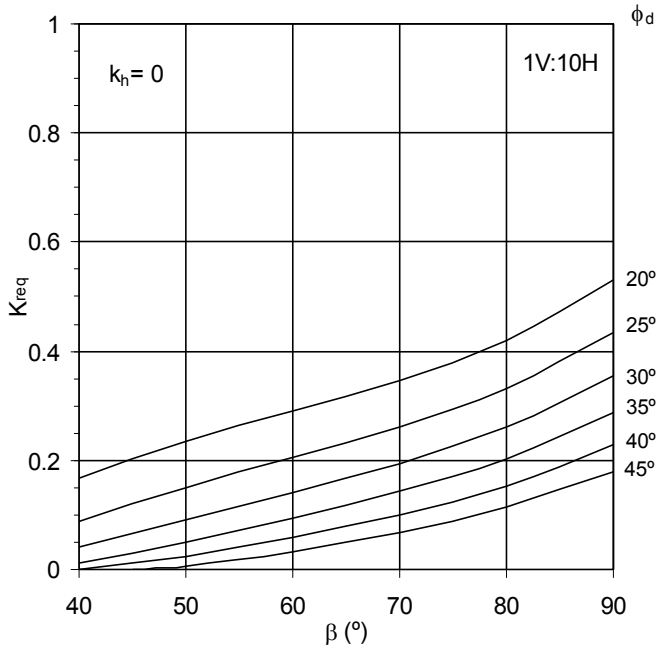

(a) Static conditions ($k_h = 0$)

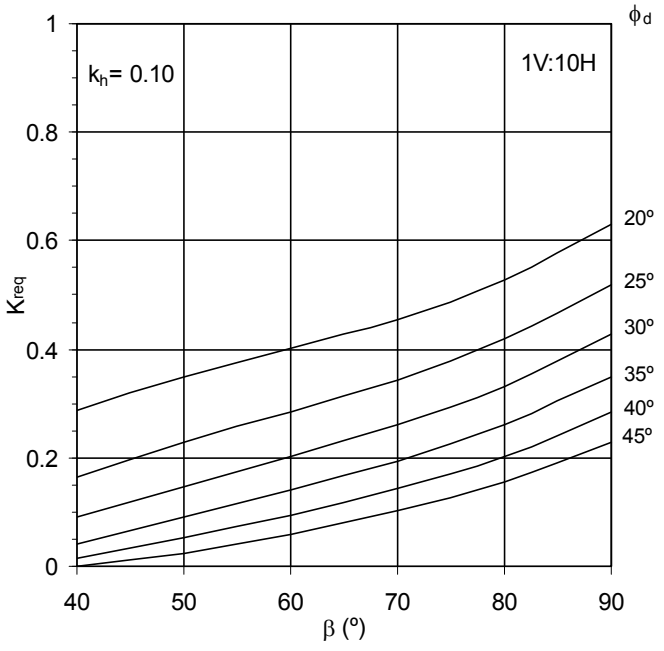

(b) $k_\eta = 0.10$

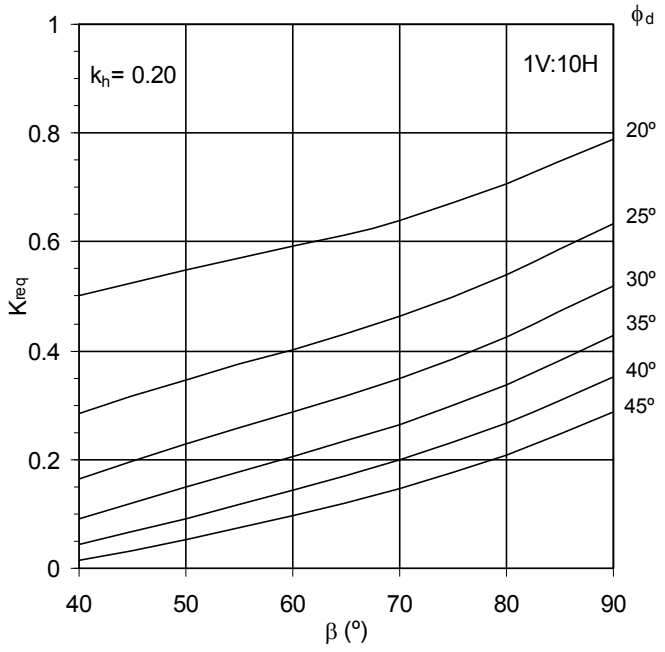

(c) $k_h = 0.20$

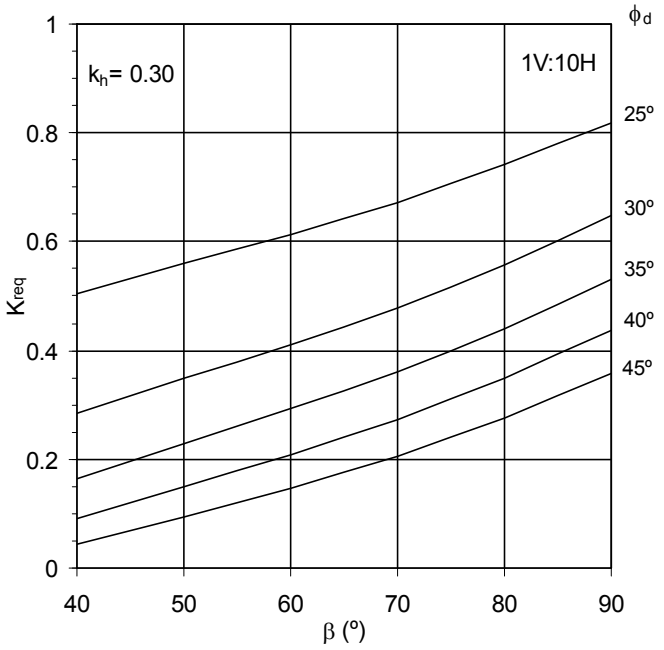

(d) $k_h = 0.30$

Fig. 9 Design charts for slopes with backslope angle, $\alpha = \tan^{-1}(1/10)$

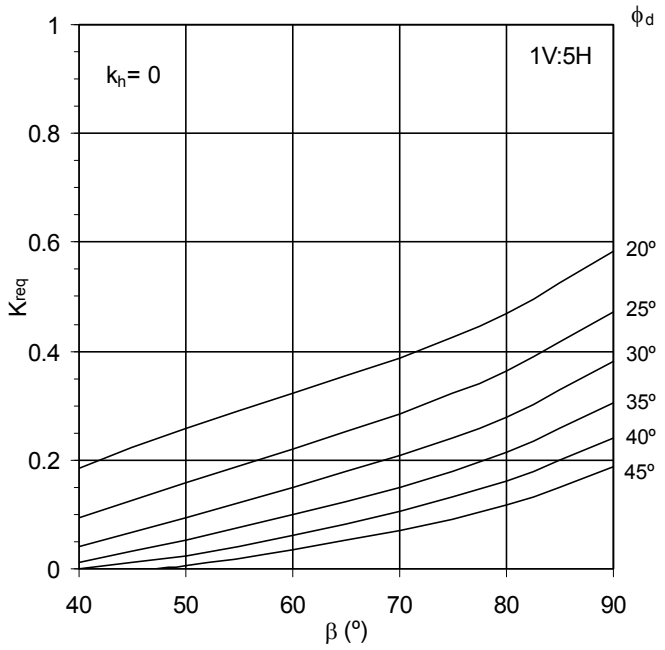

(a) Static conditions ($k_h = 0$)

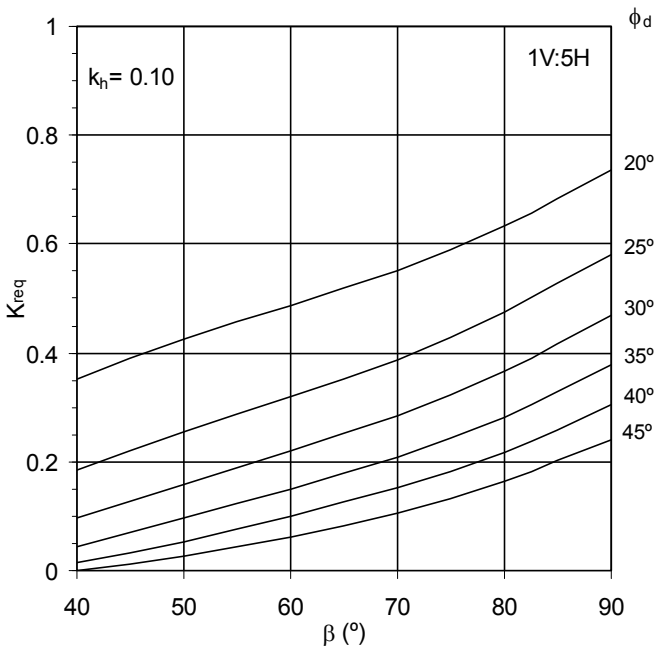

(b) $k_h = 0.10$

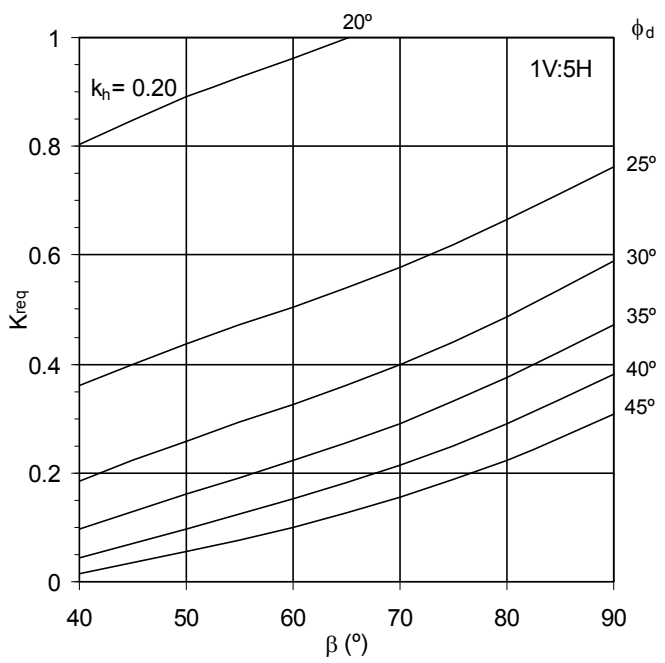

(c) $k_h = 0.20$

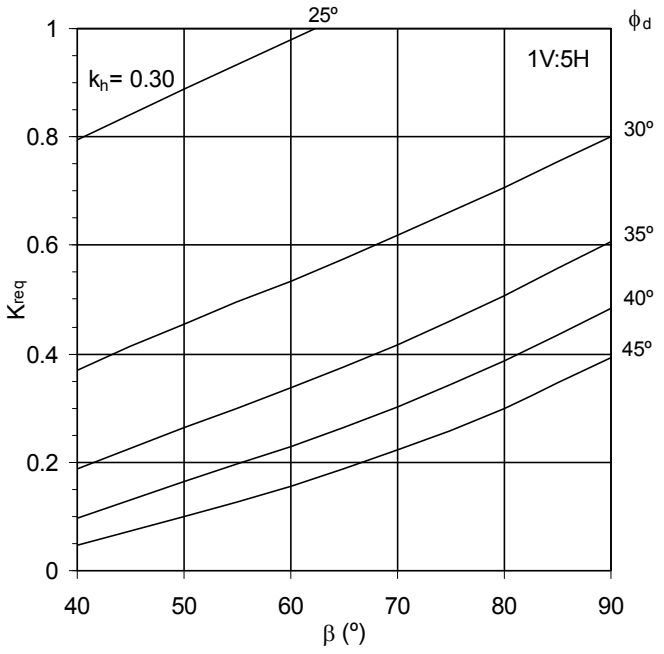

(d) $k_h = 0.30$

Fig. 10 Design charts for slopes with backslope angle, $\alpha = \tan^{-1}(1/5)$

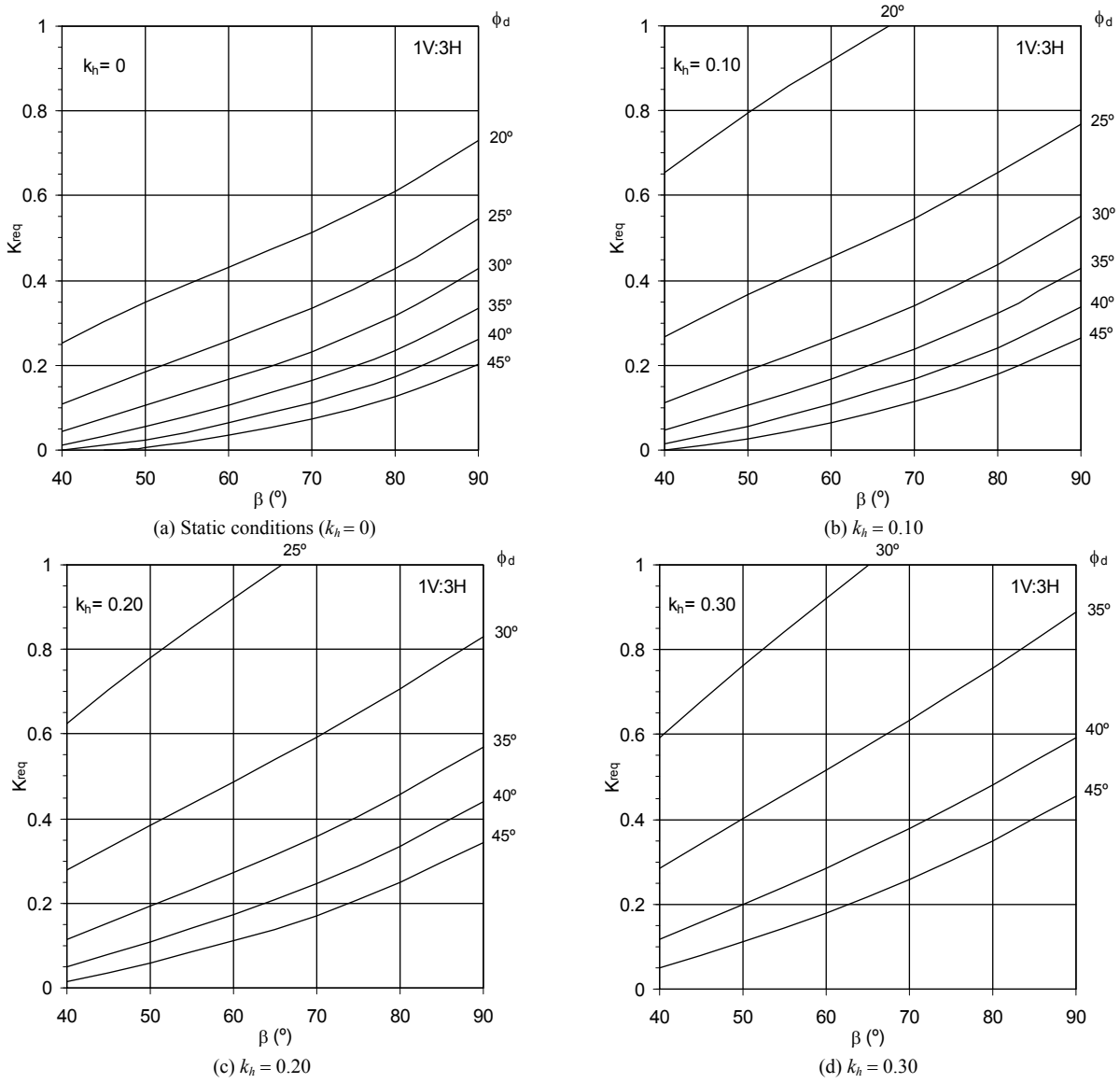

(a) Static conditions ($k_h = 0$)

(b) $k_h = 0.10$

(c) $k_h = 0.20$

(d) $k_h = 0.30$

Fig. 11 Design charts for slopes with backslope angle, $\alpha = \tan^{-1}$ (1/3)

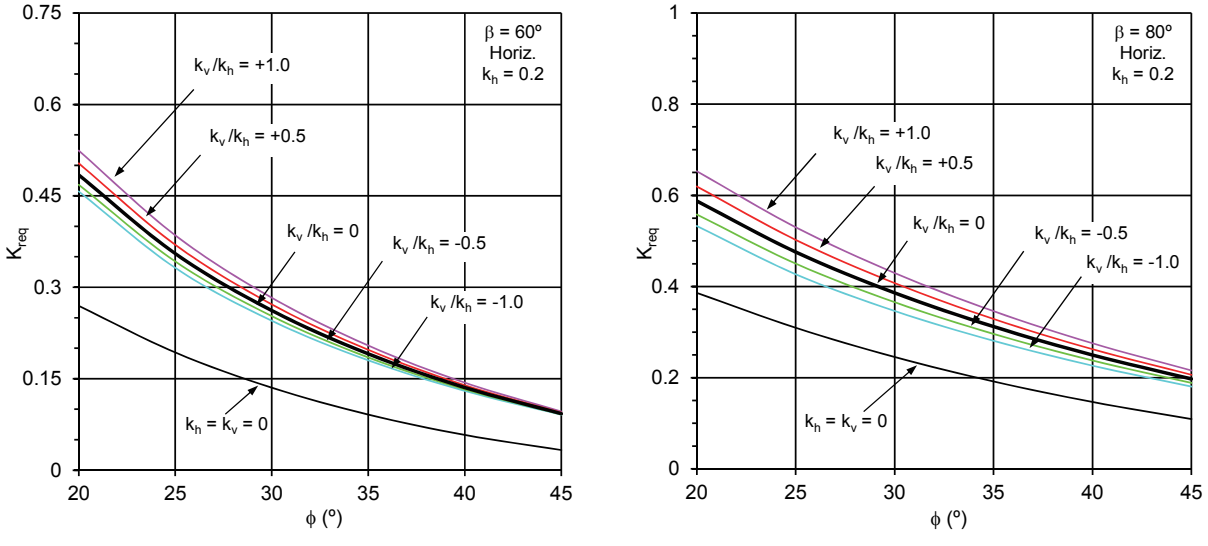

(a) β = 60°

(b) β = 80°

Fig. 12 Effect of the vertical seismic coefficient, k_v , on the earth pressure coefficient for horizontal backslope ($k_h = 0.2$)

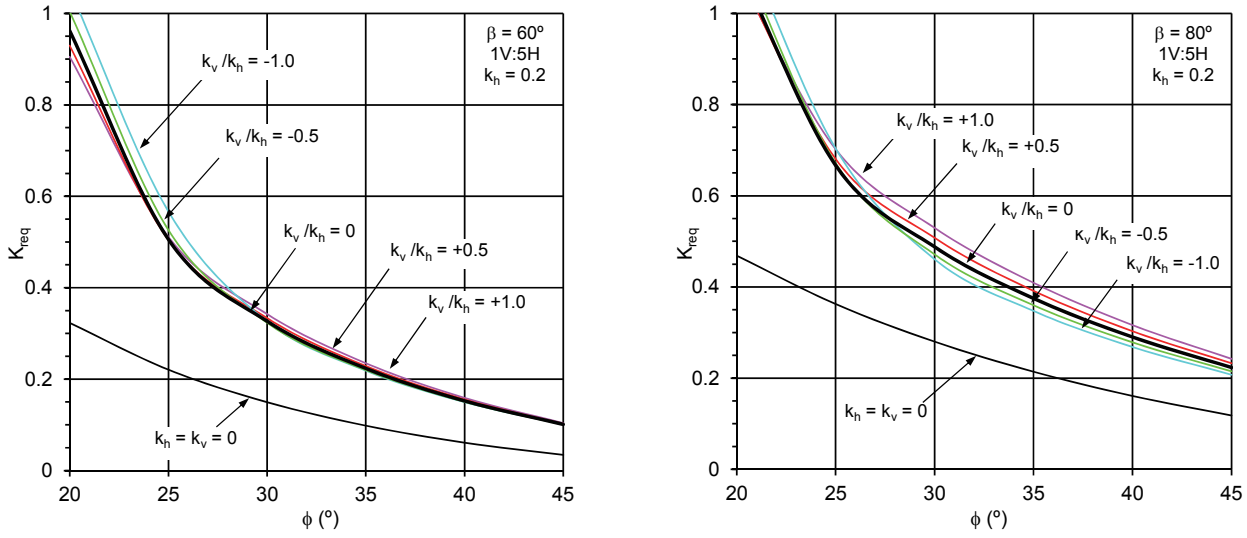

(a) β = 60°, α = tan^{-1} (1/5) (b) β = 80°, α = tan^{-1} (1/5)

Fig. 13 Effect of the vertical seismic coefficient, k_v , on the earth pressure coefficient ($k_h = 0.2$)

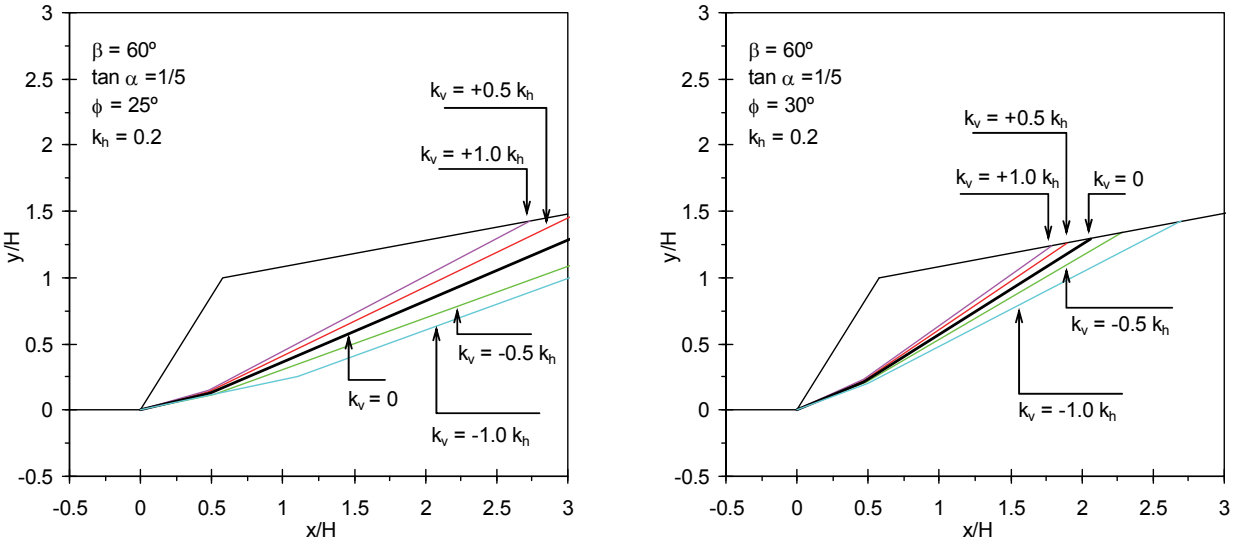

(a) ϕ = 25° (b) ϕ = 30°

Fig. 14 Effect of the vertical seismic coefficient, k_v , on critical failure surfaces for backslope angle, α = tan^{-1} (1/5), and slope angle, β = 60°

It is worth mentioning that for the two slope angles under analysis (β = 60° and β = 80°), the maximum increase in the required force for equilibrium induced by the vertical seismic action is around 11% and occurs for structures with horizontal backslope.

Even if the definition of the minimum length of reinforcements is outside the scope of this paper, it is important to point out that reinforcements' length has an utmost importance in the stability of geosynthetic reinforced structures.

It is unfeasible, from the practical point of view, to define the minimum reinforcement length under seismic loading conditions by the critical failure surfaces illustrated in Figs. 6 and 14, particularly when a seismic inertial force acting upward ($k_v < 0$) is admitted. In such cases, a more realistic design should be carried out, through analyses that consider the available reinforcement strength at each layer. If the available reinforcement strength at the lowest reinforcement layers is greater than the minimum required value (see Eq. (5)), the mobilization of the strength of the reinforcement layers placed at lower depths is not necessary to achieve the equilibrium (stability).

4. CONCLUSIONS

This paper presented a pseudo static-limit equilibrium approach, which uses a two-part wedge failure mechanism, to achieve the required reinforcement strength of geosynthetics in reinforced slopes with inclined backslope.

Design charts and potential failure surfaces were presented. Given the slope angle, the backslope angle, the internal friction angle of the soil and the horizontal and vertical seismic coefficients, it is possible to obtain an equivalent earth pressure coefficient to estimate the required force to design a stable slope.

Based on the analysis and interpretation of the results presented herein, the following conclusions can be drawn:

1. The effect of the backslope on the required force for slope equilibrium under static conditions decreases with the soil friction angle and is more significant for steeper slopes.
2. When the slope angle is not close to 90° (vertical facing), Coulomb's earth pressure theory and Mononobe-Okabe theory should not be used to estimate the required force for equilibrium, since they do not provided the critical failure surface.
3. The increase of the required force for slope equilibrium induced by the seismic loading, comparatively to the one requested in static conditions, grows with the backfill internal friction angle and has greater significance for flatter slopes.
4. The effects of the vertical component of seismic loading on the required force for slope equilibrium are not very significant. However the upwards vertical inertial forces should not be neglected particularly for soils with low shear strength.

It should be noted that the study herein presented focuses mainly on internal failure due to tensile over-stress of reinforcements. The location of failure surfaces, an important issue for the internal stability against pullout failure, is also illustrated through the paper. Theoretically the anchorage length of each geosynthetic layer must extend beyond the critical failure surface to resist pullout failure. However, for seismic design it is unfeasible to define the minimum reinforcement length by these critical failure surfaces. In such cases, the available strength at each reinforcement layer should be considered for determining the minimum length.

ACKNOWLEDGEMENTS

The author would like to thank the financial support of Portuguese Science and Technology Foundation (FCT) and FEDER, Research FCOMP-01-0124-FEDER-028842-PTDC/ECM-GEO/0622/2012.

NOMENCLATURES

g	acceleration of gravity (m/s^2)
H	height of structure (m)
H	horizontal distance in the backslope (m)
V	vertical distance in the backslope (m)
H_1	horizontal component of inter-wedge force (Fig. 1) (kN/m)
k_h	horizontal seismic coefficient (dimensionless)
K_{req}	equivalent earth pressure coefficient (dimensionless)
K_{ae}	Mononobe-Okabe earth pressure coefficient (dimensionless)
K_v	vertical seismic coefficient (dimensionless)
N_1	normal force acting at the base of wedge 1 (kN/m)
N_2	normal force acting at the base of wedge 2 (kN/m)
P_{ae}	required force for equilibrium (kN/m)
S_1	shear force acting at the base of wedge 1 assuming full mobilization of soil shear strength (kN/m)
S_2	shear force acting at the base of wedge 2 assuming full mobilization of soil shear strength (kN/m)
S_v	vertical spacing between reinforcement layers (m)
T_d	design value of the reinforcement strength (kN/m)
V_1	vertical component of inter-wedge force (kN/m)
W	weight of failure mass (kN/m)
W_1	weight of wedge 1 (kN/m)
W_2	weight of wedge 2 (kN/m)
z	depth of reinforcement layer (m)
α	backslope angle (°)
β	slope angle (°)
ϕ	soil internal friction angle (°)
ϕ_d	design value of backfill internal friction angle (°)
γ	backfill unit weight (kN/m^3)
λ	inter-wedge mobilized shear stress ratio (dimensionless)
θ_1	angle to the horizontal of potential failure surface at the base of wedge 1 (°)
θ_2	angle to the horizontal of potential failure surface at the base of wedge 2 (°)

REFERENCES

AASHTO (2002). *Standard Specifications for Highway Bridges*. 17th Ed., Association of State Highway and Transportation Officials, Washington DC, 689 p.

Ausilio, E., Conte, E., and Dente, G. (2000). "Seismic stability analysis of reinforced slopes." *Soil Dynamics and Earthquake Engineering*, **19**, 159–172.

Basha, B. and Basudhar, P. (2010). "Pseudo static seismic stability analysis of reinforced soil structures." *Geotechnical and Geological Engineering*, **28**(6), 745–762.

Bathurst, R. J. and Hatami, K. (1998). "Seismic response analysis of a geosynthetic-reinforced soil retaining wall." *Geosynthetics International*, **5**(1-2), 127–166.

Coulomb, C. A. (1776). "Essai sur une application des règles des maximis et minimis à quelques problèmes de statique relatifs à l' architecture." *Memoires de l' Academie Royale pres Divers Savants*, **7**, Paris.

FHWA (2010). *Design and Construction of Mechanically Stabilized Earth Walls and Reinforced Soil Slopes, Geotechnical Engineering Circular No. 11, FHWA-NHI-10-024*. Federal Highway Administration, US Department of Transportation, Washington D.C.

Ghanbari, A. and Ahmadabadi, M. (2010). "New analytical procedure for seismic analysis of reinforced retaining wall with cohesive-frictional backfill." *Geosynthetics International*, **17**(6), 364–379.

Jewell, R. A. (1989). "Revised design charts for steep reinforced slopes." *Proceedings of Symposium Reinforced Embankments: Theory and Practice*, Thomas Telford, 65p.

JRTRI (1999). *Manual on Design and Construction of Geosynthetic-Reinforced Soil Retaining Walls*. Japan Railway Technical Research Institute, English version: Tanslated by Ling, H.I & Tatsuoka, F.

Ling, H. I. and Leshchinsky, D. (1998). "Effects of vertical acceleration on seismic design of geosynthetic-reinforced soil structures." *Geotechnique*, **48**(3), 347–373.

Ling, H. I., Leshchinsky, D., and Perry, E. B. (1997). "Seismic design and performance of geosynthetic-reinforced soil structures." *Geotechnique*, **47**(5), 933–952.

Michalowski, R. L. (1998). "Soil reinforcement for seismic design of

geotechnical structures." *Computers and Geotechnics*, **23**, 1–17.

Mononobe, N. and Matsuo, O. (1929). "On the determination of earth pressure during earthquakes." *Proceedings of World Engineering Conference*, Tokyo, **9**, 179–187.

NCMA (1998). *Segmental Retaining Wall Seismic Design Procedure. Supplement to Design Manual for Segmental Retaining Walls*. Second Ed., 1997, R.J. Bathurst, 87p.

Nouri, H., Fakher, A., and Jones, C. J. F. P. (2008). "Evaluating the effects of the magnitude and amplification of pseudo-static acceleration on reinforced soil slopes and walls using the limit equilibrium Horizontal Slices Method." *Geotextiles and Geomembranes*, **26**(3), 263–278.

Okabe, S. (1924). "General theory on earth pressure and seismic stability of retaining wall and dam." *Journal of the Japan Society of Civil Engineers*, **10**(6), 1277–1323.

Schmertmann, G. R., Chouery-Curtis, V. E., Johnson, R. D., and Bonaparte, R. (1987). "Design charts for geogrid-reinforced soil slopes." *Proceedings of Geosynthetics' 87*, New Orleans, **1**, 108–120.

Terzaghi, K. (1943). *Theoretical Soil Mechanics*. John Wiley and Sons, New York, 510 p.

Vieira, C. S. (2014). "A simplified approach to estimate the resultant force for the equilibrium of unstable slopes." *International Journal of Civil Engineering*, **12**(1), 65–71.

Vieira, C. S., Lopes, M. L., and Caldeira, L. M. (2006). "Seismic response of a geosynthetic reinforced steep slope using FLAC." *Proceedings of 4th International FLAC Symposium on Numerical Modeling in Geomechanics*, Madrid, Spain, 267–274.

Vieira, C. S., Lopes, M. L., and Caldeira, L. M. (2011). "Earth pressure coefficients for design of geosynthetic reinforced soil structures." *Geotextiles and Geomembranes*, **29**(5), 491–501.

Vieira, C. S., Lopes, M. L., and Caldeira, L. M. (2013). "Limit equilibrium analyses for internal design of geosynthetic reinforced slopes: Influence of potential failure surface and strength distribution." *Geotechnical and Geological Engineering*, **31**(4), 1123–1135.

Wright, S. G., and Duncan, J. M. (1991). *Limit Equilibrium Stability Analyses for Reinforced Slopes*. Transp. Res. Rec. 1330, Transportation Research Board, Washington, DC, 40–46.

Yang, K.-H., Zornberg, J. G., Hung, W.-Y., and Lawson, C. R. (2011). "Location of failure plane and design considerations for narrow geosynthetic reinforced soil wall systems." *Journal of GeoEngineering*, **6**(1), 27–40.

Yang, K.-H., Utomo, P., and Liu, T.-L. (2013). "Evaluation of force-equilibrium and deformation-based design approaches for predicting reinforcement loads within geosynthetic reinforced soil structures." *Journal of GeoEngineering*, **8**(2), 41–54.